

# Oxidative Transformation of Leucocyanidin by Anthocyanidin Synthase from *Vitis vinifera* Leads Only to Quercetin

Jia-rong Zhang,<sup>†</sup> Claudine Trossat-Magnin,<sup>‡</sup> Katell Bathany,<sup>†</sup> Serge Delrot,<sup>‡</sup> and Jean Chaudière\*<sup>†</sup>

<sup>†</sup>Chimie et Biologie des Membranes et des Nano-objets (CBMN, UMR 5248), Université de Bordeaux, 33615 Pessac, France

<sup>‡</sup>Institut des Sciences de la Vigne et du Vin (ISVV, UMR 1287), Université de Bordeaux, 33140 Villenave d'Ornon, France

**S** Supporting Information

**ABSTRACT:** Anthocyanidin synthase from *Vitis vinifera* (VvANS) catalyzes the *in vitro* transformation of the natural isomer of leucocyanidin, 2R,3S,4S-*cis*-leucocyanidin, into 2R,4S-flavan-3,3,4-triol ( $[M + H]^+$ ,  $m/z$  323) and quercetin. The C<sub>3</sub>-hydroxylation product 2R,4S-flavan-3,3,4-triol is first produced and its C<sub>3</sub>,C<sub>4</sub>-dehydration product is in tautomeric equilibrium with (+)-dihydroquercetin. The latter undergoes a second VvANS-catalyzed C<sub>3</sub>-hydroxylation leading to a 4-keto-2R-flavan-3,3-gem-diol which upon dehydration gives quercetin. The unnatural isomer of leucocyanidin, 2R,3S,4R-*trans*-leucocyanidin, is similarly transformed into quercetin upon C<sub>3</sub>,C<sub>4</sub>-dehydration, but unlike 3,4-*cis*-leucocyanidin, it also undergoes some C<sub>2</sub>,C<sub>3</sub>-dehydration followed by an acid-catalyzed hydroxyl group extrusion at C<sub>4</sub> to give traces of cyanidin. Overall, the C<sub>3</sub>,C<sub>4</sub>-*trans* isomer of leucocyanidin is transformed into 2R,4R-flavan-3,3,4-triol ( $M + 1$ ,  $m/z$  323), (+)-DHQ, (–)-epiDHQ, quercetin, and traces of cyanidin. Our data bring the first direct observation of 3,4-*cis*-leucocyanidin- and 3,4-*trans*-leucocyanidin-derived 3,3-gem-diols, supporting the idea that the generic function of ANS is to catalyze the C<sub>3</sub>-hydroxylation of its substrates. No cyanidin is produced with the natural *cis* isomer of leucocyanidin, and only traces with the unnatural *trans* isomer, which suggests that anthocyanidin synthase requires other substrate(s) for the *in vivo* formation of anthocyanidins.

**KEYWORDS:** leucoanthocyanidin dioxygenase, anthocyanidin synthase, *Vitis vinifera*, 2-oxoglutarate, ascorbate, leucocyanidin, reaction mechanism

## INTRODUCTION

Anthocyanins, glycoside derivatives of unstable anthocyanidins, are the most abundant water-soluble pigments in plants, fulfilling many important ecological and physiological functions, such as recruitment of pollinators and seed dispersers, light screening photoprotection, and free radical scavenging.<sup>1–5</sup> Anthocyanins are mostly used as dyes in the food industry,<sup>6</sup> and further developments are expected with the acylated anthocyanins which have improved color stability.<sup>7,8</sup> Numerous studies have also demonstrated that several anthocyanins have pharmacological properties that may be beneficial for human health,<sup>6,9</sup> including cardioprotective,<sup>10</sup> antithrombotic,<sup>11</sup> antidiabetic,<sup>12</sup> anti-inflammatory,<sup>13</sup> or anti-tumor activities.<sup>14–16</sup>

All these observations have stimulated the development of new strategies to design anthocyanin biosynthetic reactors,<sup>17–19</sup> with the implicit assumption that the current understanding of anthocyanidin and anthocyanin biosynthesis is correct.

The biosynthetic pathways of flavonoids have been thoroughly studied and most of the enzymes involved have been presumably identified,<sup>20</sup> but the biosynthetic pathways of anthocyanidins may not be fully understood.

Anthocyanidin synthase (ANS, EC 1.14.11.19), which is believed to catalyze the last step of anthocyanidin biosynthesis, is also known as leucoanthocyanidin dioxygenase (LDOX), with the underlying assumption that leucoanthocyanidins are the major sources of anthocyanidins.

ANS is a member of the 2-oxoglutarate-dependent dioxygenase superfamily, and as initially shown with the

recombinant enzyme from *Perilla frutescens*,<sup>21</sup> it requires 2-oxoglutarate, Fe(II), and ascorbate for its activity. In this work, it was shown that significant albeit small amounts of anthocyanidins could be produced by the enzyme from either leucocyanidin or leucopelargonidin. This was in apparent agreement with previous genomic data which supported the specific requirement of the corresponding gene in anthocyanidin biosynthesis,<sup>22–24</sup> and also with the fact that feeding plants with 2,3-*cis*-leucocyanidin had been shown to stimulate anthocyanin production.<sup>23</sup> For years, ANS has therefore been assumed to be responsible for the *in vivo* transformation of colorless leucoanthocyanidins (2R,3S,4S) into colored anthocyanidins. However, this ANS-catalyzed transformation of leucoanthocyanidins has never been confirmed to be a major source of anthocyanidins *in vivo*. Moreover, ANS from *Arabidopsis thaliana* (AtANS) was actually shown to catalyze the oxidation of the natural stereoisomer of leucocyanidin (LCD) mostly into products other than cyanidin.<sup>25,26</sup>

The ANS gene has been cloned in several plants, and the enzyme characterized using distinct polyphenolic substrates,<sup>24,27–29</sup> and it was concluded that ANS was actually able to catalyze the oxidative transformation of (+)-dihydroquercetin (DHQ), (+)-catechin, and naringenin *in vitro*. It was hypothesized that the initial ANS-catalyzed step was a

**Received:** December 13, 2018

**Revised:** February 12, 2019

**Accepted:** March 13, 2019

**Published:** March 13, 2019

hydroxylation at C<sub>3</sub>,<sup>25,26,30,31</sup> but no C<sub>3</sub>-hydroxylated product was detected in the enzymatic reaction mixture at that time.

As part of our general study of recombinant ANS from *Vitis vinifera* (VvANS), we report here the direct detection of monohydroxylated products of 3,4-*cis* and 3,4-*trans* LCDs (M + 1, m/z 323), and we show that they are 3,3-gem-diols resulting from enzymatic C<sub>3</sub>-hydroxylation, based on the analysis of their degradation products. The final degradation product of the 3,3-gem-diol derived from natural 3,4-*cis* LCD is quercetin, and our data do not support an ANS-catalyzed transformation of this natural isomer into cyanidin.

## MATERIALS AND METHODS

**Chemicals.** (+)-Sodium L-ascorbate (≥98%), α-ketoglutaric acid sodium salt (≥98%), iron(II) sulfate heptahydrate (≥99%), catalase from bovine liver (powder), (+)-taxifolin (2R,3S-dihydroquercetin or (+)-DHQ, ≥85%), quercetin (≥95%), and methanol (HPLC grade) were all purchased from Sigma-Aldrich. Cyanidin chloride (≥96%) was purchased from Extrasynthèse (France). Thrombin from bovine plasma (dry powder, GE Healthcare) was dissolved in ice-cold PBS buffer (pH 7.4) to a final concentration of 1 unit/μL and stored in small aliquots at -80 °C.

**Cloning and Expression of Recombinant VvANS in *Escherichia coli*.** The full-length cDNA of VvANS (GenBank accession number ABV82967.1) was amplified from a cDNA library of Cabernet sauvignon berries (*Vitis vinifera*, postveraison) and cloned into pDONR201 Gateway-compatible vector (Invitrogen), sequenced, and subcloned into the pGGWA destination vector [accession no. EU680839]<sup>32</sup> using LR clonase (Invitrogen) following the manufacturer's protocol.

The resulting expression plasmid was finally transformed into the *Escherichia coli* BL21(DE3) strain (Novagen) for protein expression. The recombinant bacteria were first grown at 37 °C in 30 mL 2XYT medium supplemented with 1% (v/v) glycerol and 100 μg/mL ampicillin for 18 h at 200 rpm, the bacterial preculture was then transferred into 2 L 2XYT medium supplemented with 1% (v/v) glycerol and 100 μg/mL ampicillin and growth continued at 37 °C under shaking (200 rpm) until an A<sub>600</sub> of approximately 1.0 was reached. Induction of protein expression was initiated by the addition of 1 mM IPTG, followed by a further incubation at 30 °C for 16 h under shaking at 200 rpm.

**Production of Untagged VvANS.** Protein purification was carried out using Protino Ni-TED resin (MACHEREY-NAGEL, Germany) according to the instructions provided by the manufacturer, with minor modifications. The cells harvested from *E. coli* expression culture by centrifugation (4 °C, 5000g, 30 min) were resuspended in ice-cold LEW buffer (lysis–equilibration–wash, 50 mM NaH<sub>2</sub>PO<sub>4</sub>, 300 mM NaCl, pH 8.0) using 1 g wet cell weight for 2 mL LEW buffer. The suspension was stirred on ice for 30 min after addition of 1 mg/mL lysozyme (from hen egg-white, Sigma) and sonicated (Branson Digital Sonifier) on ice for 5 min at 25% of maximal power (15 s burst with a 30 s cooling period). Cellular debris were removed by centrifugation (4 °C, 8600g, 30 min), and the supernatant was filtered through a 0.45 μm membrane (Whatman syringe filter, GE Healthcare Life Sciences). The cleared bacterial lysate was immediately loaded onto the gravity-flow IMAC column prepared using the Protino Ni-TED resin and the recombinant protein was eluted using elution buffer (50 mM NaH<sub>2</sub>PO<sub>4</sub>, 300 mM NaCl, 250 mM imidazole, pH 8.0). After concentration by centrifugation (Vivaspin 20, 30 kDa, Sartorius) and buffer exchange with a gel-filtration cartridge (PD-10 desalting column, GE Healthcare), the purified recombinant protein was stored in PBS buffer (pH 7.3) for further tag removal.

After dilution of the purified recombinant protein sample with PBS buffer to a final concentration of 2 mg/mL (Bradford method), tag removal was initiated by adding 15 units/mL thrombin and the mixture was then incubated at 22 °C for 16 h under shaking at 160 rpm. The cleaved His<sub>6</sub>-GST tag was removed first on another column

of Protino Ni-TED resin, and the untagged protein was collected together with thrombin in the flow-through.

Thrombin present in the collected untagged protein sample was finally removed with *p*-aminobenzamidine–agarose (*p*-ABA, Sigma, 200 μL suspension for 50 units of thrombin). After addition of *p*-ABA, the mixture was gently shaken at room temperature for 30 min and passed through a filter of 50 μm pore size, and the thrombin-free VvANS was recovered. The untagged protein was concentrated (Vivaspin 20, 10 kDa, Sartorius), and the protein buffer was exchanged for the final storage buffer (20 mM MES, 500 mM NaCl, 10% (v/v) glycerol, pH 6.5) using a PD-10 gel-filtration column.

**Enzyme Assays.** (+)-2,3-*trans*-3,4-*cis*-Leucocyanidin and its 3,4-*trans* isomer were synthesized and stored as previously described<sup>33</sup> and then used as substrates of VvANS, and the products were analyzed by HPLC and mass spectrometry (MS).

**Reverse-Phase HPLC Analysis.** The reaction mixture (2 mL, final volume) contained 20 mM ammonium acetate, 20 mM NaCl, 2 mM ascorbate, 1 mM 2-oxoglutarate, 10 μM FeSO<sub>4</sub>, 0.1 mg/mL catalase, and 10<sup>-6</sup> M VvANS (≈ 80.6 μg), pH 6.3 (at 35 °C). After a preincubation of the reaction mixture at 35 °C for 5 min, the reaction was triggered by the addition of 100 μM LCD, and then incubated at 35 °C for 30 min under gentle magnetic stirring. A 100 μL portion of the reaction mixture was then analyzed by reverse-phase HPLC using an Atlantis C18 column (5 μm, 4.6 mm × 250 mm; Waters) thermostated at 30 °C. Products were separated using a 25 min linear gradient from 20 to 90% B under a flow rate of 1 mL/min and detected at 280 nm. Solvent A was water-acidified with 0.1% (v/v) trifluoroacetic acid (TFA), and solvent B was methanol-acidified with 0.1% TFA.

**Tandem Mass Spectrometry (MS/MS) Analysis.** Elution fractions of the HPLC chromatogram were collected and analyzed by electrospray ionization tandem mass spectrometry (ESI-MS/MS) which was performed on a Q-ToF Premier mass spectrometer (Waters) equipped with an electrospray ionization source (ESI) and a time-of-flight (TOF) analyzer. The samples were infused with a syringe pump into the ESI source at a flow rate of 5 μL/min. MS analyses were performed in positive ion mode as previously described.<sup>33</sup> MS/MS analyses were carried out using argon as collision gas with a collision energy of 3 to 30 eV and a collision cell gas flow of 0.47 L/min. The full scan MS/MS spectra were measured from 100 to 800 m/z.

Methanolic solutions of 2 mM (+)-DHQ, quercetin, and cyanidin were freshly prepared and used as references.

**Chemical Synthesis and Chiral HPLC Analysis of (+)-epi-DHQ.** The chemical synthesis of (+)-epiDHQ was carried out using the procedure described by Kiehlmann and Li<sup>34</sup> and checked by NMR.<sup>30</sup> Upon a 12 h incubation at 75 °C of 1 mM (+)-DHQ in 1 mL methanol/H<sub>2</sub>O (50/50, v/v) containing 0.5 M HCl, the only product formed, (+)-epiDHQ, was purified by HPLC using the Atlantis C18 column. The collected samples were pooled and completely dried out by rotary-evaporation at 20 °C and the resulting (+)-epiDHQ was finally redissolved in hexane/ethanol (70/30, v/v) for chiral HPLC analysis.

Chiral HPLC analysis was performed on a Chiralcel OJ-H column (5 μm, 4.6 mm × 250 mm; Daicel) following the procedure described by Gargouri et al.<sup>35</sup> The stereoisomer of DHQ was isocratically eluted with hexane/ethanol (70/30, v/v) at room temperature under a flow rate of 0.5 mL/min and detected at 214 nm. A 100 μM of (+)-DHQ in hexane/ethanol (70/30, v/v) was used as a reference.

## RESULTS

**Enzyme Production.** The expression plasmid pGGWA codes for an N-terminal His<sub>6</sub>-GST tagged VvANS, in which VvANS is linked to the tag by a thrombin cleavage site (Figure S1). The His<sub>6</sub>-GST tag and thrombin were entirely removed from VvANS, as shown by the SDS-PAGE analysis (Figure S2).

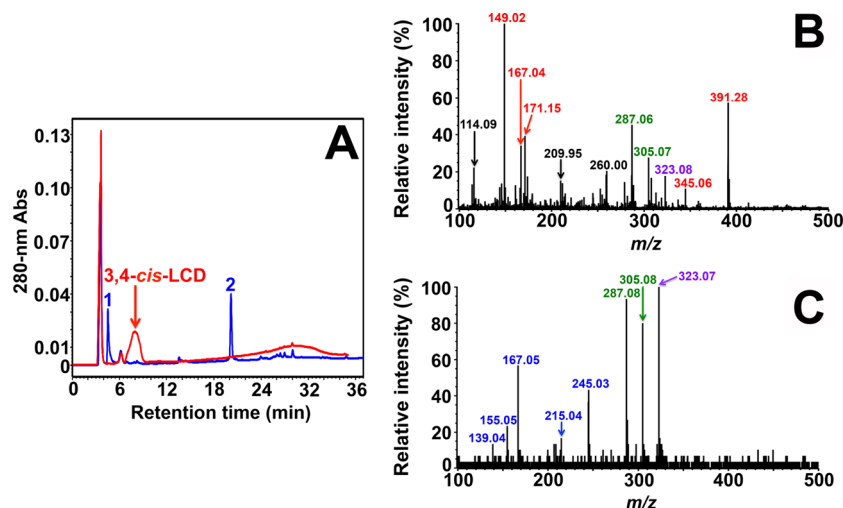


**Figure 1.** Characterization of ANS products of 3,4-*cis*-LCD. (A) Reverse-phase HPLC analysis. The nonenzymatic degradation products of 3,4-*cis*-LCD (8.0 min) are shown in red, and its enzymatic degradation products are shown in blue. (B) MS analysis of the collected peak 1.  $m/z$  149, 171, and 391 are contaminant ions derived from phthalate or plasticizer in methanol extracts.<sup>36</sup> (C) MS/MS fragmentation of the ion with  $m/z$  323 observed in part B.

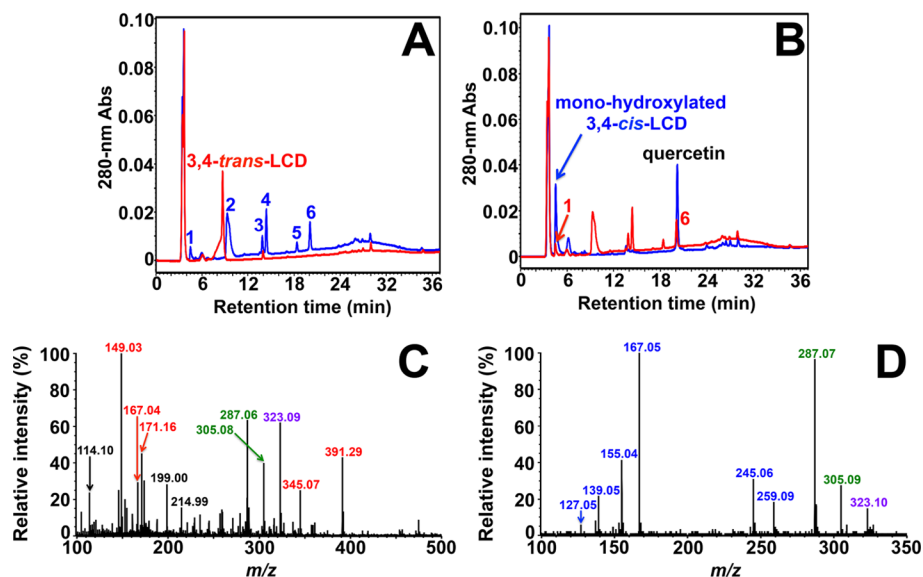


**Figure 2.** Characterization of ANS products of 3,4-*trans*-LCD. (A) Reverse-phase HPLC analysis. The nonenzymatic degradation products of 3,4-*trans*-LCD (8.7 min) are shown in red, and its enzymatic degradation products are shown in blue. (B) Reverse-phase HPLC analysis. The enzymatic degradation products of 3,4-*trans*-LCD are shown in red and that of 3,4-*cis*-LCD is shown in blue. (C) MS analysis of the collected peak 2. (D) MS/MS fragmentation of the  $[M + H]^+$  ion with  $m/z$  323 observed in part C.

At the end of the purification process, VvANS was analyzed by ESI-MS in order to check its integrity. As shown in Figure S3, the full-length protein (observed average mass: 40338.0 Da; theoretical average mass: 40337.38 Da) is exclusively present in the sample, indicating that there is no loss of amino acid and no protein cleavage during purification.

The purified VvANS is stable in the selected storage buffer and could be kept at 4 °C up to 1 month or at −20 °C in small aliquots for several months.

Approximately 30–50 mg of recombinant His<sub>6</sub>-GST-VvANS could be obtained from 2 L of culture medium. Upon tag removal, a final yield of 5–7.5 mg of VvANS per L could be achieved.

**Enzyme Assays.** Incubation of 3,4-*cis*-LCD with VvANS. Enzyme assays were first carried out using the natural isomer of

leucocyanidin (3,4-*cis*) as substrate, and a control experiment was performed in the absence of VvANS (Figure 1A, in red).

As shown in Figure 1A (in blue), the peak of 3,4-*cis*-LCD disappeared upon incubation with VvANS, and two products (peaks 1 and 2) were observed.

The identification of these two products by MS/MS was subsequently carried out. As shown in Figure 1B, three ions with  $m/z$  287, 305, and 323 are observed on the MS spectrum of peak 1. Further MS/MS analysis of the ion with  $m/z$  323 (Figure 1C) shows that it is mainly broken down into three fragment ions with  $m/z$  167, 287, and 305 at the very low collision energy (3 eV) which was selected, suggesting that the three ions with  $m/z$  167, 287, and 305 observed in Figure 1B were already due to the fragmentation of  $m/z$  323. The latter is therefore most likely the  $[M + H]^+$  ion of peak 1. Therefore, the product visualized as peak 1 (Figure 1A) would have a

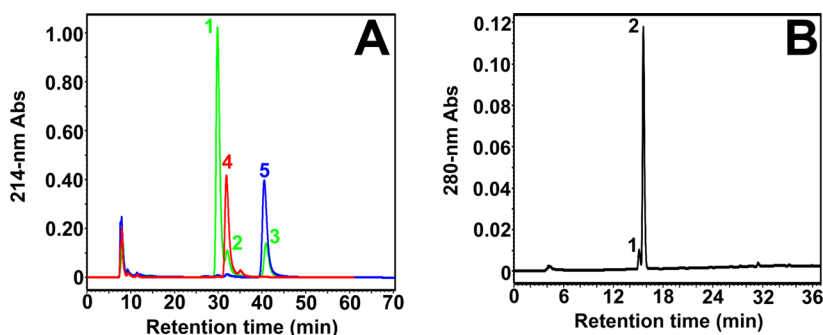


**Figure 3.** HPLC analysis of the three stereoisomers of DHQ. (A) Chiral HPLC overlay chromatogram of the sample of (+)-epiDHQ (in green), (+)-DHQ (in red), and the unknown stereoisomer (in blue). The peak observed around 10 min is found in the three cases, and it cannot therefore be considered as a polyphenolic structure. (B) Reverse-phase HPLC analysis of the final sample of (+)-epiDHQ. Peak 1 is (+)-DHQ (residual) and peak 2 is (+)-epiDHQ.

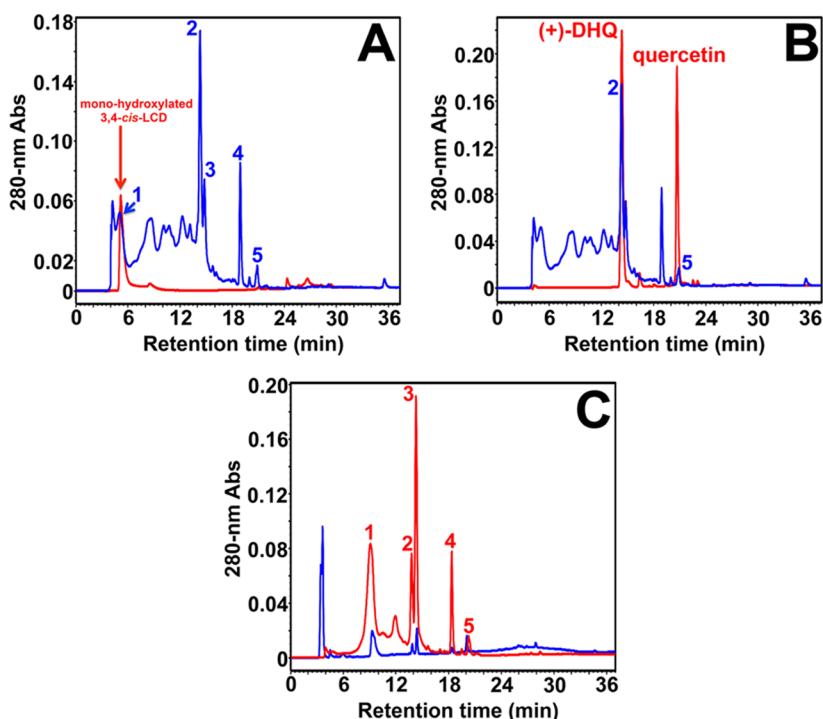


**Figure 4.** Reverse-phase HPLC analysis of the nonenzymatic degradation products of the monohydroxylated 3,4-*cis*- and 3,4-*trans*-LCD. (A) HPLC overlay chromatogram of the sample of the monohydroxylated 3,4-*cis*-LCD before (in red) and after (in blue) freeze-drying. (B) HPLC overlay chromatogram of the nonenzymatic degradation products of the monohydroxylated 3,4-*cis*-LCD (in blue) and the mixture of the commercial standards of 50  $\mu\text{M}$  (+)-DHQ and quercetin (in red). (C) HPLC overlay chromatogram of enzymatic degradation products of 3,4-*trans*-LCD (in blue) and nonenzymatic degradation products of monohydroxylated 3,4-*trans*-LCD (in red).

molecular weight of 322 Da which corresponds to a monohydroxylation product of 3,4-*cis*-LCD (306 + 16 Da). In addition, the ion with  $m/z$  345 in Figure 1B corresponds to the  $[\text{M} + \text{Na}]^+$  ion derived from  $m/z$  323.

The product visualized as peak 2 (Figure 1A) was unambiguously identified by MS/MS as quercetin, using commercial quercetin as external standard (Figure S4).

**Incubation of 3,4-*trans*-LCD with VvANS.** With 3,4-*trans*-LCD as substrate, six possible enzymatic products were observed after incubation with VvANS (Figure 2A, in blue), implying that this non-natural isomer also behaves as a substrate, but its enzymatic transformation is more complex. As shown in Figure 2B, red peaks 1 and 6 can be assigned to the monohydroxylated 3,4-*cis*-LCD and quercetin, respectively, by comparison with the two products of 3,4-*cis*-LCD (Figure 2B, in blue). In fact, monohydroxylated 3,4-*cis*-LCD was

probably formed from the enzymatic transformation of approximately 13% 3,4-*cis*-LCD present as contaminant in the stock solution of 3,4-*trans*-LCD.<sup>33</sup>

The analysis of the other four products was again carried out by means of MS/MS. Peak 2 corresponds to the monohydroxylation product of 3,4-*trans*-LCD with a molecular weight of 322 Da ( $[\text{M} + \text{H}]^+$ ,  $m/z$  323), based on its MS and MS/MS spectra (Figure 2C and D) which were very similar to those of the monohydroxylated 3,4-*cis*-LCD (Figure 1B and C).

Products visualized as peaks 3 and 4 (very close) were undistinguishable from (+)-DHQ by MS/MS using commercial (+)-DHQ as external standard (Figure S5), suggesting that they are two stereoisomers, and a subsequent HPLC analysis (Figure S6) revealed that peak 3 is (+)-DHQ. Therefore, peak 4 is a stereoisomer of (+)-DHQ (2*R*,3*R*-DHQ), which could

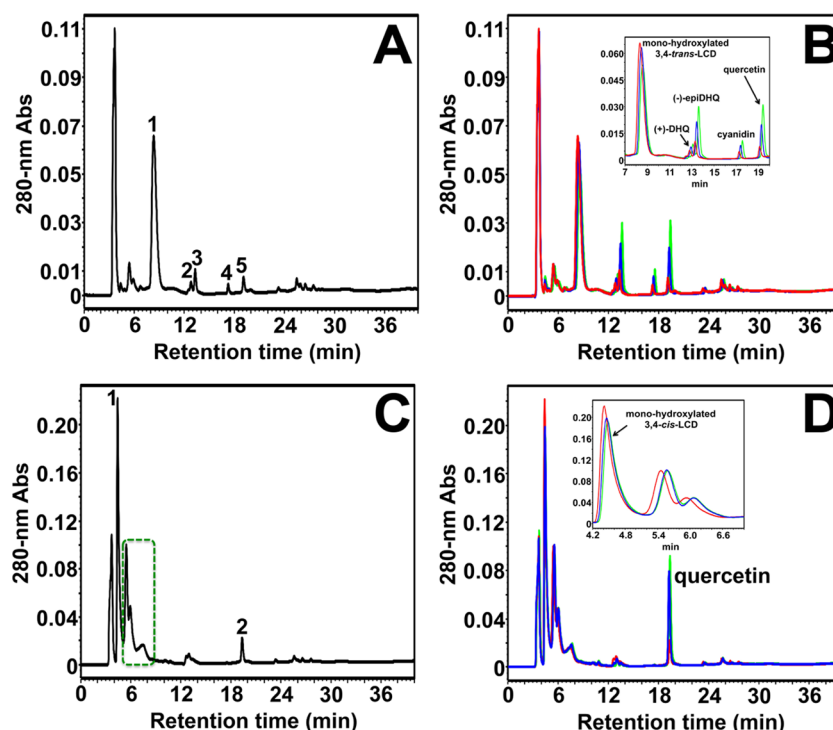


**Figure 5.** Reverse-phase HPLC monitoring of the enzymatic transformation of 3,4-*trans*- and 3,4-*cis*-LCD performed at 22 °C. (A) After 30 min incubation of 3,4-*trans*-LCD with VvANS. (B) Overlay of HPLC chromatograms of the reaction mixture (100  $\mu$ L) analyzed at 30 (red), 80 (blue), and 120 min (green) after the addition of 3,4-*trans*-LCD. (inset) Magnified chromatogram between 7.0 and 20.0 min. (C) After 30 min incubation of 3,4-*cis*-LCD with VvANS. The boxed peaks which are also observed in part D are contaminating degradation products of 3,4-*cis*-LCD. (D) Overlay of HPLC chromatograms of the reaction mixture (100  $\mu$ L) analyzed at 30 (red), 80 (blue), and 120 min (green) after the addition of 3,4-*cis*-LCD. (inset) Magnified chromatogram between 4.2 and 7.0 min.

be either (+)-epiDHQ (2*S*,3*R*-DHQ) or (–)-epiDHQ (2*R*,3*S*-DHQ), but not (–)-DHQ (2*S*,3*S*-DHQ), because (+)-DHQ and (–)-DHQ could not be separated in our conditions. As described later, further chiral HPLC analysis was carried out in order to confirm our assignment of peak 4.

Peak 5 was unambiguously assigned to cyanidin by MS/MS using commercial cyanidin as external standard (Figure S7).

**Confirmation of the Observed Stereoisomer of (+)-DHQ by Chiral HPLC Analysis.** (+)-epiDHQ and (–)-epiDHQ are not commercially available, but we successfully synthesized (+)-epiDHQ as mentioned earlier. The observed stereoisomer of (+)-DHQ (peak 4 in Figure 2A) was purified and redissolved in hexane/ethanol (70/30, v/v) as described for (+)-epiDHQ in Materials and Methods. As shown in Figure 3A, injection of this sample on the Chiralcel OJ-H column gives a peak at 40.5 min (blue peak 5). This peak 5 is well separated from (+)-epiDHQ (green peak 1, 29.9 min), indicating that it is (–)-epiDHQ. In addition, the small green peak 2 (32.1 min) was assigned to (+)-DHQ using the commercial standard of (+)-DHQ (red peak 4, 31.9 min), and this (+)-DHQ is actually a residual contaminant of the purified sample of (+)-epiDHQ (Figure 3B). Another small green peak 3 (40.9 min) was assigned to (–)-epiDHQ (blue peak 5, 40.5 min), which probably resulted from the C<sub>3</sub> keto–enol tautomerization of (+)-DHQ.<sup>30</sup>

**Nonenzymatic Degradation Products of the Monohydroxylated 3,4-*cis*- and 3,4-*trans*-LCD.** Our attempts to produce a pure freeze-dried sample of each of these two compounds for structural identification by NMR failed, because they were not stable and were degraded during freeze-drying. The corresponding degradation products were

further analyzed. After purification of the monohydroxylated 3,4-*cis*-LCD by reverse-phase HPLC (peak 1 in Figure 1A), only one major peak was observed on the HPLC chromatogram of the purified sample (Figure 4A, in red). This sample was lyophilized and redissolved in methanol/H<sub>2</sub>O (50/50, v/v). Reverse-phase HPLC analysis (Figure 4A, in blue) showed that this monohydroxylated 3,4-*cis*-LCD (blue peak 1) had decomposed into several byproducts (peaks 2–5). As shown in Figure 4B, peaks 2 and 5 were respectively assigned to (+)-DHQ and quercetin using commercial standards. Peak 3 (Figure 5A) was assigned to (–)-epiDHQ by chiral HPLC analysis using the Chiralcel OJ-H column, and peak 4 (Figure 4A) was assigned to cyanidin based on MS/MS analysis.

The sample of monohydroxylated 3,4-*trans*-LCD was lyophilized and analyzed in the same way. As shown in Figure 4C (in red), five peaks were observed, which were respectively assigned to the monohydroxylated 3,4-*trans*-LCD (residual), (+)-DHQ, (–)-epiDHQ, cyanidin, and quercetin when compared with the products obtained from the enzymatic transformation of 3,4-*trans*-LCD (Figure 4C, in blue). The last four compounds resulted from the nonenzymatic degradation of the first one during freeze-drying, and one should note that they were also obtained from the enzymatic transformation of 3,4-*trans*-LCD (Figure 2A).

**Reverse-Phase HPLC Monitoring of the Enzymatic Reactions Performed at 22 °C.** The results of our investigation of the nonenzymatic degradation of monohydroxylated 3,4-*trans*-LCD cast some doubt about the enzymatic origin of all the products of 3,4-*trans*-LCD (Figure 2A). Therefore, the enzymatic transformation of 3,4-*trans*-LCD was performed at a lower temperature (22 °C), with the

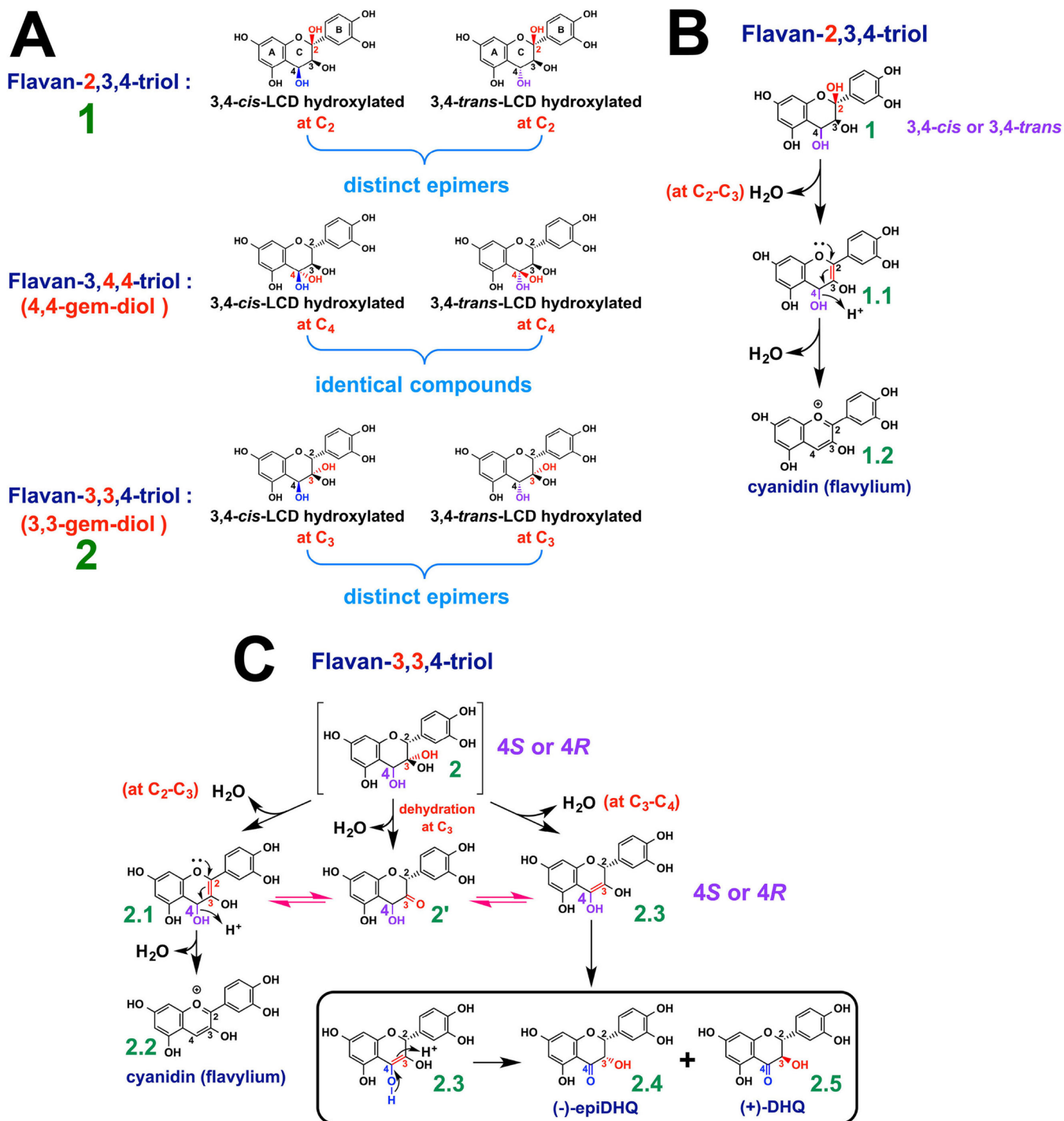


**Figure 6.** Hypothetical nonenzymatic degradation pathways of putative hydroxylation products of 3,4-*cis*- and 3,4-*trans*-leucocyanidin. (A) Hydroxylation products of 3,4-*cis*- and 3,4-*trans*-LCD may result from hydroxylation at C<sub>2</sub>, C<sub>3</sub>, or C<sub>4</sub>. (B) Proposed nonenzymatic degradation pathway of the flavan-2,3,4-triol. (C) Proposed nonenzymatic degradation pathway of the flavan-3,3,4-triol. The box shows the formation of (-)-epiDHQ and (+)-DHQ through keto-enol tautomerization of the intermediate flav-3-en-3,4-diol 2.3.

aim to reduce the nonenzymatic degradation of monohydroxylated 3,4-*trans*-LCD.

As shown in Figure 5A, after 30 min incubation at 22 °C in the presence of VvANS, 3,4-*trans*-LCD was no longer observed and the same products were obtained (Figure 2). However, the monohydroxylated 3,4-*trans*-LCD (peak 1) was observed as the only major product, and the other four products (peaks 2–5) were found at trace levels. In addition, for longer incubation times, the amount of monohydroxylated 3,4-*trans*-LCD

declined and the other four products increased simultaneously (Figure 5B).

The enzymatic transformation of 3,4-*cis*-LCD was also tested at 22 °C, and a similar trend was observed. As shown in Figure 5C, monohydroxylated 3,4-*cis*-LCD (peak 1) became the major product, with traces of the other product (quercetin, peak 2). A decrease in monohydroxylated 3,4-*cis*-LCD and an increase in quercetin were also observed following longer incubation times (Figure 5D).

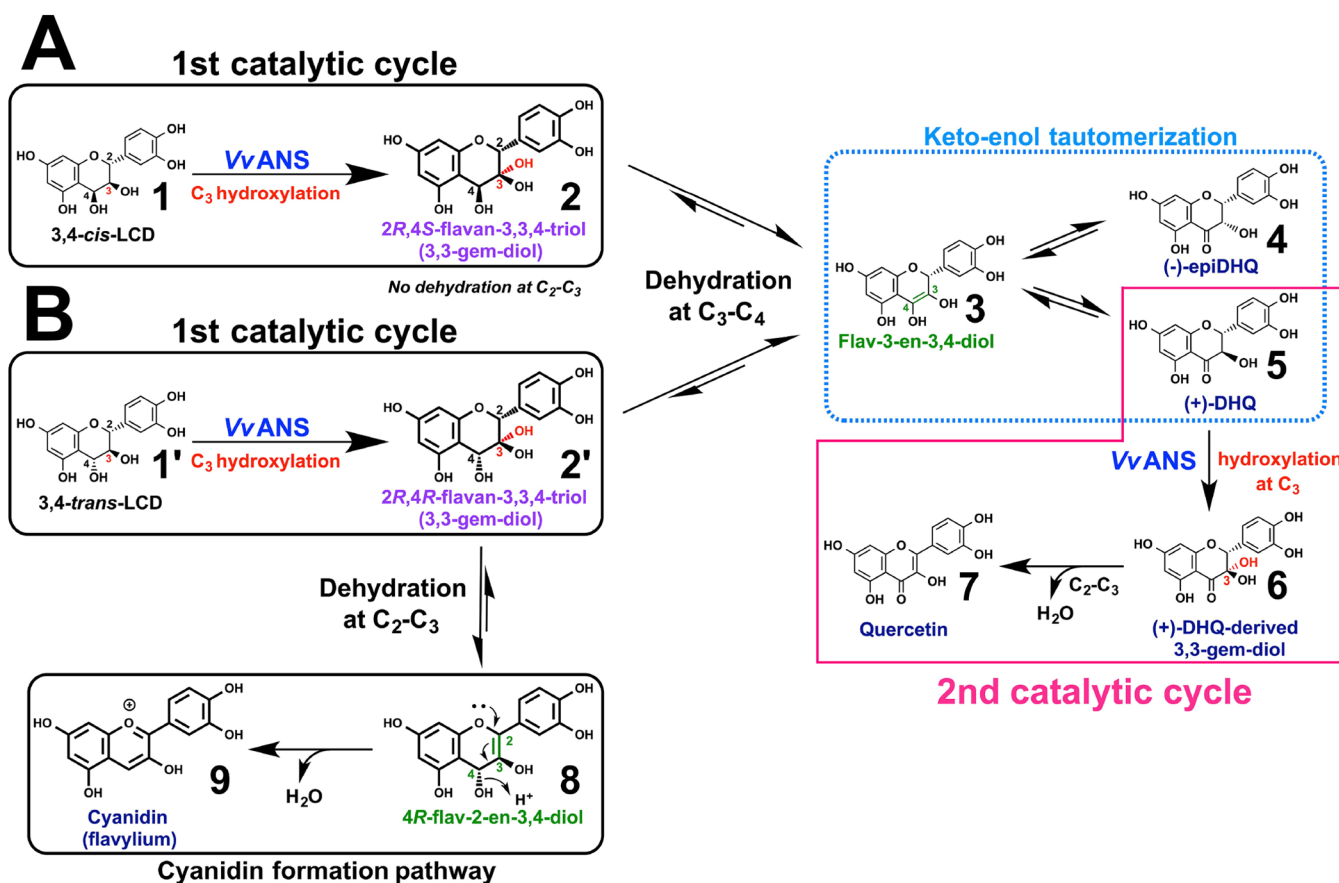


Figure 7. Proposed *in vitro* oxidation of 3,4-*cis*-LCD (A) and 3,4-*trans*-LCD (B) catalyzed by VvANS.

## DISCUSSION

**Structure of the Monohydroxylated 3,4-*cis*- and 3,4-*trans*-Leucocyanidin.** Two monohydroxylated leucocyanidins were obtained from the transformation of the corresponding stereoisomer of leucocyanidin (3,4-*cis* or 3,4-*trans*) by VvANS according to the MS and MS/MS analysis, but the hydroxylation position of these two structures could not be directly observed, because of the lack of pure sample for NMR analysis.

Hydroxylation at C<sub>2</sub>, C<sub>3</sub>, and C<sub>4</sub> of ring C may all be postulated, to yield the flavan-2,3,4-triol, flavan-3,3,4-triol (3,3-gem-diol), and flavan-3,4,4-triol (4,4-gem-diol), respectively (Figure 6A). If the hydroxylation occurred at C<sub>4</sub>, no difference would be found between the two formed flavan-3,4,4-triols, which cannot be in agreement with distinct HPLC retention times (peak 1 in Figure 1A and peak 2 in Figure 2A). The C<sub>4</sub>-hydroxylation is therefore excluded because it would give the same product, whereas the C<sub>2</sub> and C<sub>3</sub> hydroxylations are still possible because the structures would be C<sub>4</sub> epimers in all cases.

Interestingly, the nonenzymatic degradation of the putative hydroxylation products can help us to solve the problem. The observed monohydroxylated 3,4-*cis*- and 3,4-*trans*-LCD are indeed nonenzymatically degraded into three major by-products which are (+)-DHQ, (-)-epiDHQ, and cyanidin, as well as traces of quercetin. The flavan-2,3,4-triol 1 of Figure 6B could dehydrate at C<sub>2</sub>-C<sub>3</sub> by loss of the C<sub>2</sub> hydroxyl group, to yield an intermediate flav-2-en-3,4-diol 1.1, from which an acid-catalyzed dehydration step would yield cyanidin in its flavylium form 1.2.

Although cyanidin is an expected nonenzymatic degradation product of flavan-2,3,4-triol, dihydroquercetin should not be produced, which is not compatible with our results. Therefore, in addition to C<sub>4</sub> hydroxylation, the C<sub>2</sub> hydroxylation is also excluded.

The two hydroxyl groups bound to the same carbon atom (C<sub>3</sub>) of the flavan-3,3,4-triol (2, Figure 6C) can be easily converted to a carbonyl or keto group by dehydration at C<sub>3</sub>, forming an intermediate flav-3-en-3,4-diol 2', which is a tautomeric form of the flav-2-en-3,4-diol 2.1 and flav-3-en-3,4-diol 2.3. Furthermore, the intermediate flav-2-en-3,4-diol 2.1 could be directly formed from dehydration of the flavan-3,3,4-triol 2 at C<sub>2</sub>-C<sub>3</sub>, with elimination of one of the two hydroxyl groups at C<sub>3</sub>, and in this case, the formation of the cyanidin cation 2.2 could be achieved in the same way as that described on the left path of Figure 6B. As shown on the right side of Figure 6C, another dehydration of the flavan-3,3,4-triol 2 at C<sub>3</sub>-C<sub>4</sub> could also be envisaged, to yield the intermediate flav-3-en-3,4-diol 2.3, which is a tautomeric form of (-)-epiDHQ 2.4 and (+)-DHQ 2.5.

In summary, the three dehydration products of the flavan-3,3,4-triol which can be envisaged, namely cyanidin, (+)-DHQ, and (-)-epiDHQ do correspond with the three observed major byproducts of the two monohydroxylated leucocyanidins. We therefore conclude that the observed monohydroxylated 3,4-*cis*- and 3,4-*trans*-LCD are the flavan-3,3,4-triol of (2R,4S) and (2R,4R) configurations, respectively.

**Reaction Mechanism of the *in vitro* VvANS-Catalyzed Oxidation of Leucocyanidins (3,4-*cis* or 3,4-*trans*).** On the basis of our results, the most likely reaction mechanism of

the *in vitro* VvANS-catalyzed oxidation of 3,4-*cis*- and 3,4-*trans*-LCD is that of Figure 7 in which we show that two consecutive ANS-catalyzed hydroxylation steps are required to produce quercetin from each of the two isomers. The first one gives a 3,3-gem-diol (2 from 3,4-*cis*-LCD and 2' from 3,4-*trans*-LCD) which undergoes dehydration at C<sub>3</sub>–C<sub>4</sub> to flav-3-en-3,4-diol 3. The latter is in equilibrium with the 4-keto tautomers 4 and 5. Then a 3*R* secondary hydroxyl group is again available with (+)-DHQ 5 for a second hydroxylation by ANS (second catalytic cycle) to a 4-keto-3,3-gem-diol which dehydrates to quercetin. The formation of cyanidin 9 does not involve a second hydroxylation step, but requires a C<sub>2</sub>,C<sub>3</sub>-dehydration which is only observed with the triol derived from the *trans* isomer (4*R* hydroxyl group). This suggests that this C<sub>2</sub>,C<sub>3</sub>-dehydration is ANS-catalyzed and C<sub>4</sub>-stereospecific.

With 3,4-*cis*-LCD 1 (Figure 7A), two major products were initially observed when the enzymatic reaction was performed at 35 °C for 30 min (Figure 1A), which are 3,4-*cis*-LCD-derived 3,3-gem-diol (compound 2) and quercetin 7. However, compound 2 became a major product when the reaction was performed at 22 °C, and quercetin 7 was found at trace level (Figure 5C). With longer incubation times, the amount of quercetin 7 increased significantly and that of compound 2 decreased (Figure 5D), suggesting that compound 2 is the initial oxidation product from which quercetin 7 is produced. Compound 2 is unstable because of the C<sub>3</sub> gem-diol, and it is expected to dehydrate into an enediol with a double bond at C<sub>2</sub>–C<sub>3</sub> or C<sub>3</sub>–C<sub>4</sub>. An enediol with a double bond at C<sub>2</sub>–C<sub>3</sub> should yield some cyanidin 9, which is not observed with 3,4-*cis*-LCD. This means that this is a double bond at C<sub>3</sub>–C<sub>4</sub> which is obtained by dehydration, which would yield compound 3. The latter would be in equilibrium with two 4-keto tautomers, (–)-epiDHQ and (+)-DHQ, which have a CHOH available at C<sub>3</sub> where a second ANS-catalyzed hydroxylation could take place. This would produce a second 3,3-gem-diol from which the formation of quercetin 7 is indeed expected. The substrate used by VvANS for this second hydroxylation is most likely (+)-DHQ. As shown in figure S8, when (+)-DHQ is used as initial substrate, VvANS indeed produces a single product which is quercetin.<sup>37</sup>

With 3,4-*trans*-LCD 1' (Figure 7B), five products were initially observed when the enzymatic reaction was performed at 35 °C for 30 min (Figure 2A), which are 3,4-*trans*-LCD-derived 3,3-gem-diol (compound 2'), (–)-epiDHQ 4, (+)-DHQ 5, quercetin 7, and cyanidin 9. We must therefore admit that compounds 4, 5, and 7 are derived from compound 2' exactly as described for 3,4-*cis* LCD from compound 2. The keto–enol tautomerization steps of compounds 3, 4, and 5 are probably nonenzymatic since the HPLC analysis of the enzymatic products of 3,4-*trans*-LCD produced at more basic pH (7.8) showed that (+)-DHQ and (–)-epiDHQ were observed in similar amounts (Figure S9A). This would agree with the fact that the ANS-catalyzed transformation of (+)-DHQ into quercetin is negligible at this pH (Figure S9B).

In summary, when the two stereoisomers of leucocyanidin are used as substrates of VvANS, the corresponding C<sub>3</sub>-hydroxylation products, namely the 3,4-*cis*- and 3,4-*trans*-LCD-derived 3,3-gem-diols are formed. These 3,3-gem-diols are the initial oxidation products of the ANS-catalyzed oxidation of leucocyanidins, and they undergo dehydration to give the flav-2-en-3,4-diol (4*S* or 4*R*) and flav-3-en-3,4-diol.

Although our attempts to purify substantial amounts of 3,4-*cis*- and 3,4-*trans*-LCD-derived 3,3-gem-diols for NMR analysis have failed due to their insufficient stability, our mechanistic interpretations are in agreement with several independent observations. This work also clearly confirms that the natural isomer of leucocyanidin is not a significant precursor of cyanidin and that the leucoanthocyanidin dioxygenase (LDOX) activity of the enzyme is therefore unlikely to be responsible for its anthocyanidin synthase activity, at least *in vitro*. A corollary of this observation is that it will be necessary to check whether the ANS from *Perilla frutescens* on which the original hypothesis was based<sup>21</sup> does produce significant amounts of cyanidin from the natural 3,4-*cis*-leucocyanidin or only from some contaminating 3,4-*trans*-isomer. The authors had used leucocyanidin and leucopelargonidin from commercial source, and they were aware of this potential problem since they wrote<sup>21</sup> that it would be difficult to determine which epimer was the true substrate of ANS, given the ease of spontaneous isomerization at C<sub>4</sub>.

Here we used a recombinant vVANS, and it cannot be formally excluded that it could be devoid of some important post-translational modification, but we must underline that this recombinant enzyme does produce significant amounts of cyanidin from (+)-catechin.<sup>37</sup> If the lack of transformation of 3,4-*cis*-leucoanthocyanidins is confirmed with ANS from various sources, this will imply that leucoanthocyanidins may be transformed by an enzyme situated between DFR and ANS into products which are then efficiently transformed by ANS into anthocyanidins. This enzyme would most likely be leucoanthocyanidin reductase (LAR) since one of its products, namely (+)-catechin has been shown to be transformed into significant amounts of cyanidin by all ANS investigated to date,<sup>27–29</sup> including Vv-ANS in our hands.<sup>37</sup> In fact, it was shown that ANS did not appear to provide an efficient conversion of leucoanthocyanidins to anthocyanidins in *E. coli* transfected with flavanone 3β-hydroxylase, dihydroflavonol reductase, and ANS,<sup>38</sup> and catechin has been used as an alternative and far more efficient substrate of ANS upon transfection of *E. coli* with the additional LAR gene.<sup>39–41</sup>

## ■ ASSOCIATED CONTENT

### 📄 Supporting Information

The Supporting Information is available free of charge on the ACS Publications website at DOI: 10.1021/acs.jafc.8b06968.

Figure S1. pHGGWA expression plasmid constructed using the Gateway technology. Figure S2. SDS-PAGE analysis of the recombinant VvANS at each step of the purification. Figure S3. ESI-MS analysis of the untagged VvANS. Figure S4. MS and MS/MS analysis of the product visualized as peak 2 in Figure 1A. Figure S5. MS and MS/MS analysis of the products visualized as peaks 3 and 4 in Figure 2A. Figure S6. Reverse-phase HPLC confirmation of the product visualized as peak 3 in Figure 2A. Figure S7. MS and MS/MS analysis of the product visualized as peak 5 in Figure 2A. Figure S8. Identification of the ANS product of (+)-DHQ. Figure S9. Transformation of 3,4-*trans*-LCD (A) and (+)-DHQ (B) by VvANS at pH 7.8 (PDF)

## ■ AUTHOR INFORMATION

## Corresponding Author

\*Tel.: +33 (0)6 63 07 53 48. Fax: +33 (0)5 40 00 24 38. E-mail: [jean.chaudiere@u-bordeaux.fr](mailto:jean.chaudiere@u-bordeaux.fr).

ORCID 

Jean Chaudière: 0000-0002-9420-1473

## Notes

The authors declare no competing financial interest.

## ■ ACKNOWLEDGMENTS

We would like to thank our colleague Claude Manigand for his technical advice with the chiral HPLC analysis. J.-r.Z. gratefully acknowledges a three-year funding PhD scholarship from the department of Bioengineering (Qilu University of Technology, China).

## ■ REFERENCES

- (1) Kong, J. M.; Chia, L. S.; Goh, N. K.; Chia, T. F.; Brouillard, R. Analysis and biological activities of anthocyanins. *Phytochemistry* **2003**, *64*, 923–933.
- (2) Steyn, W. J.; Wand, S. J. E.; Holcroft, D. M.; Jacobs, G. Anthocyanins in vegetative tissues: a proposed unified function in photoprotection. *New Phytol.* **2002**, *155*, 349–361.
- (3) Ferreira da Silva, P. F.; Paulo, L.; Barbařina, A.; Elisei, F.; Quina, F. H.; Maćanita, A. L. Photoprotection and the photophysics of acylated anthocyanins. *Chem. - Eur. J.* **2012**, *18*, 3736–3744.
- (4) Petrusa, E.; Braidot, E.; Zancani, M.; Peresson, C.; Bertolini, A.; Patui, S.; Vianello, A. Plant flavonoids – Biosynthesis, transport and involvement in stress responses. *Int. J. Mol. Sci.* **2013**, *14*, 14950–14973.
- (5) Goupy, P.; Bautista-Ortin, A. B.; Fulcrand, H.; Dangles, O. Antioxidant activity of wine pigments derived from anthocyanins: hydrogen transfer reactions to the DPPH radical and inhibition of the heme-induced peroxidation of linoleic acid. *J. Agric. Food Chem.* **2009**, *57*, 5762–5770.
- (6) Khoo, H. E.; Azlan, A.; Tang, S. T.; Lim, S. M. Anthocyanidins and anthocyanins: colored pigments as food, pharmaceutical ingredients, and the potential health benefits. *Food Nutr. Res.* **2017**, *61*, 1361779.
- (7) Giusti, M. M.; Wrolstad, R. E. Acylated anthocyanins from edible sources and their applications in food systems. *Biochem. Eng. J.* **2003**, *14*, 217–225.
- (8) Zhao, C. L.; Yu, Y. Q.; Chen, Z. J.; Wen, G. S.; Wei, F. G.; Zheng, Q.; Wang, C. D.; Xiao, X. L. Stability-increasing effects of anthocyanin glycosyl acylation. *Food Chem.* **2017**, *214*, 119–128.
- (9) Li, D.; Wang, P.; Luo, Y.; Zhao, M.; Chen, F. Health benefits of anthocyanins and molecular mechanisms: update from recent decade. *Crit. Rev. Food Sci. Nutr.* **2017**, *57*, 1729–1741.
- (10) Liobikas, J.; Skemiene, K.; Trumbeckaite, S.; Borutaite, V. Anthocyanins in cardioprotection: A path through mitochondria. *Pharmacol. Res.* **2016**, *113*, 808–815.
- (11) Aiyer, H. S.; Warri, A. M.; Woode, D. R.; Hilakivi-Clarke, L.; Clarke, R. Anthocyanins in obesity-associated thrombogenesis. Influence of berry polyphenols on receptor signaling and cell-death pathways: implications for breast cancer prevention. *J. Agric. Food Chem.* **2012**, *60*, 5693–5708.
- (12) Belwal, T.; Nabavi, S. F.; Nabavi, S. M.; Habtemariam, S. Dietary anthocyanins and insulin resistance: when food becomes a medicine. *Nutrients* **2017**, *9*, 1111.
- (13) He, Y.; Hu, Y.; Jiang, X.; Chen, T.; Ma, Y.; Wu, S.; Sun, J.; Jiao, R.; Li, X.; Deng, L.; Bai, W. Cyanidin-3-O-glucoside inhibits the UVB-induced ROS/COX-2 pathway in HaCaT cells. *J. Photochem. Photobiol., B* **2017**, *177*, 24–31.
- (14) Wang, L. S.; Stoner, G. D. Anthocyanins and their role in cancer prevention. *Cancer Lett.* **2008**, *269*, 281–290.
- (15) Fimognari, C.; Lenzi, M.; Hrelia, P. Chemoprevention of cancer by isothiocyanates and anthocyanins: mechanisms of action and structure-activity relationship. *Curr. Med. Chem.* **2008**, *15*, 440–447.
- (16) Lin, B. W.; Gong, C. C.; Song, H. F.; Cui, Y. Y. Effects of anthocyanins on the prevention and treatment of cancer. *Br. J. Pharmacol.* **2017**, *174*, 1226–1243.
- (17) Fernandes, I.; Azevedo, J.; Faria, A.; Calhau, C.; de Freitas, V.; Mateus, N. Enzymatic hemisynthesis of metabolites and conjugates of anthocyanins. *J. Agric. Food Chem.* **2009**, *57*, 735–745.
- (18) Zha, J.; Koffas, M. A. G. Production of anthocyanins in metabolically engineered microorganism: Current status and perspectives. *Synth. Syst. Biotechnol.* **2017**, *2*, 259–266.
- (19) Appelhagen, I.; Wulff-Vester, A. K.; Wendell, M.; Hvoslef-Eide, A. K.; Russell, J.; Oertel, A.; Martens, S.; Mock, H. P.; Martin, C.; Matros, A. Colour bio-factories: Towards scale-up production of anthocyanins in plant cell cultures. *Metab. Eng.* **2018**, *48*, 218–232.
- (20) Tohge, T.; Perez de Souza, L.; Fernie, A. R. Current understanding of the pathways of flavonoid biosynthesis in model and crop plants. *J. Exp. Bot.* **2017**, *68*, 4013–4028.
- (21) Saito, K.; Kobayashi, M.; Gong, Z. Z.; Yamazaki, M.; Tanaka, Y. Direct evidence for anthocyanidin synthase as a 2-oxoglutarate-dependent oxygenase: molecular cloning and functional expression of cDNA from a red form of *Perilla frutescens*. *Plant J.* **1999**, *17*, 181–189.
- (22) Menssen, A.; Höhmann, S.; Martin, W.; Schnable, P. S.; Peterson, P. A.; Saedler, H.; Gierl, A. The En/Spm transposable element of *Zea mays* contains splice sites at the termini generating a novel intron from a dSpm element in the A2 gene. *EMBO J.* **1990**, *9*, 3051–3057.
- (23) Martin, C.; Prescott, A.; Mackay, S.; Bartlett, J.; Vrijlandt, E. Control of anthocyanidin biosynthesis in flowers of *Antirrhinum majus*. *Plant J.* **1991**, *1*, 37–49.
- (24) Weiss, D.; van der Luit, A. H.; Kroon, J. T. M.; Mol, J. N. M.; Kooter, J. M. The petunia homologue of the *Antirrhinum majus candi* and *Zea mays A2* flavonoid genes; homology to flavanone 3-hydroxylase and ethylene-forming enzyme. *Plant Mol. Biol.* **1993**, *22*, 893–897.
- (25) Turnbull, J. J.; Sobey, W. J.; Aplin, R. T.; Hassan, A.; Firmin, J. L.; Schofield, C. J.; Prescott, A. G. Are anthocyanidins the immediate products of anthocyanidin synthase? *Chem. Commun.* **2000**, 2473–2474.
- (26) Turnbull, J. J.; Nagle, M. J.; Seibel, J. F.; Welford, R. W. D.; Grant, G. H.; Schofield, C. J. The C-4 stereochemistry of leucocyanidin substrates for anthocyanidin synthase affects product selectivity. *Bioorg. Med. Chem. Lett.* **2003**, *13*, 3853–3857.
- (27) Nakajima, J. I.; Tanaka, Y.; Yamazaki, M.; Saito, K. Reaction mechanism from leucoanthocyanidin to anthocyanidin 3-glucoside, a key reaction for coloring in anthocyanin biosynthesis. *J. Biol. Chem.* **2001**, *276*, 25797–25803.
- (28) Welford, R. W. D.; Clifton, I. J.; Turnbull, J. J.; Wilson, S. C.; Schofield, C. J. Structural and mechanistic studies on anthocyanidin synthase catalysed oxidation of flavanone substrates: the effect of C-2 stereochemistry on product selectivity and mechanism. *Org. Biomol. Chem.* **2005**, *3*, 3117–3126.
- (29) Wellmann, F.; Griesser, M.; Schwab, W.; Martens, S.; Eisenreich, W.; Matern, U.; Lukaćin, R. Anthocyanidin synthase from *Gerbera hybrida* catalyzes the conversion of (+)-catechin to cyanidin and a novel procyanidin. *FEBS Lett.* **2006**, *580*, 1642–1648.
- (30) Welford, R. W. D.; Turnbull, J. J.; Claridge, T. D. W.; Prescott, A. G.; Schofield, C. J. Evidence for oxidation at C-3 of the flavonoid C-ring during anthocyanidin biosynthesis. *Chem. Commun.* **2001**, 1828–1829.
- (31) Turnbull, J. J.; Nakajima, J. I.; Welford, R. W. D.; Yamazaki, M.; Saito, K.; Schofield, C. J. Mechanistic studies on three 2-oxoglutarate-dependent oxygenases of flavonoid biosynthesis. *J. Biol. Chem.* **2004**, *279*, 1206–1216.
- (32) Busso, D.; Delagoutte-Busso, B.; Moras, D. Construction of a set Gateway-based destination vectors for high-throughput cloning

and expression screening in *Escherichia coli*. *Anal. Biochem.* **2005**, *343*, 313–321.

(33) Zhang, J. R.; Tolchard, J.; Bathany, K.; Langlois d'Estaintot, B.; Chaudière, J. Production of 3,4-*cis*- and 3,4-*trans*-leucocyanidin and their distinct MS/MS fragmentation patterns. *J. Agric. Food Chem.* **2018**, *66*, 351–358.

(34) Kiehlmann, E.; Li, E. P. M. Isomerization of dihydroquercetin. *J. Nat. Prod.* **1995**, *58*, 450–455.

(35) Gargouri, M.; Manigand, C.; Maugé, C.; Granier, T.; Langlois d'Estaintot, B.; Cala, O.; Pianet, I.; Bathany, K.; Chaudière, J.; Gallois, B. Structure and epimerase activity of anthocyanidin reductase from *Vitis vinifera*. *Acta Crystallogr., Sect. D: Biol. Crystallogr.* **2009**, *65*, 989–1000.

(36) Keller, B. O.; Sui, J.; Young, A. B.; Whittal, R. M. Interferences and contaminants encountered in modern mass spectrometry. *Anal. Chim. Acta* **2008**, *627*, 71–81.

(37) Zhang, J. R. Etude de l'anthocyanidine synthase de *Vitis vinifera*: substrats polyphénoliques et mécanismes réactionnels. PhD Dissertation, Bordeaux University, 2017.

(38) Yan, Y.; Chemler, J.; Huang, L.; Martens, S.; Koffas, M. A. Metabolic engineering of anthocyanin biosynthesis in *Escherichia coli*. *Appl. Environ. Microbiol.* **2005**, *71* (7), 3617–23.

(39) Zhao, S.; Jones, J. A.; Lachance, D. M.; Bhan, N.; Khalidi, O.; Venkataraman, S.; Wang, Z.; Koffas, M. A. G. Improvement of catechin production in *Escherichia coli* through combinatorial metabolic engineering. *Metab. Eng.* **2015**, *28*, 43–53.

(40) Lim, C. G.; Wong, L.; Bhan, N.; Dvora, H.; Xu, P.; Venkiteswaran, S.; Koffas, M. A. Development of a recombinant *Escherichia coli* strain for overproduction of the plant pigment anthocyanin. *Appl. Environ. Microbiol.* **2015**, *81* (18), 6276–84.

(41) Jones, J. A.; Vernacchio, V. R.; Collins, S. M.; Shirke, A. N.; Xiu, Y.; Englaender, J. A.; Cress, B. F.; McCutcheon, C. C.; Linhardt, R. J.; Gross, R. A.; Koffas, M. A. G. Complete biosynthesis of anthocyanins using *E. coli* polycultures. *mBio* **2017**, DOI: 10.1128/mBio.00621-17.